
Journal of Biological Physics **28:** 637–653, 2002.

Deterministic versus Stochastic Models for Circadian Rhythms

D. GONZE, J. HALLOY and A. GOLDBETER*
Unité de Chronobiologie Théorique, Faculté des Sciences, Université Libre de Bruxelles, Campus Plaine, C.P. 231, B-1050 Brussels, Belgium
(**Author for correspondence, e-mail: agoldbet@ulb.ac.be*)

Abstract. Circadian rhythms which occur with a period close to 24 h in nearly all living organisms originate from the negative autoregulation of gene expression. Deterministic models based on genetic regulatory processes account for the occurrence of circadian rhythms in constant environmental conditions (e.g. constant darkness), for entrainment of these rhythms by light-dark cycles, and for their phase-shifting by light pulses. At low numbers of protein and mRNA molecules, it becomes necessary to resort to stochastic simulations to assess the influence of molecular noise on circadian oscillations. We address the effect of molecular noise by considering two stochastic versions of a core model for circadian rhythms. The deterministic version of this core model was previously proposed for circadian oscillations of the PER protein in *Drosophila* and of the FRQ protein in *Neurospora.* In the first, non-developed version of the stochastic model, we introduce molecular noise without decomposing the deterministic mechanism into detailed reaction steps while in the second, developed version we carry out such a detailed decomposition. Numerical simulations of the two stochastic versions of the model are performed by means of the Gillespie method. We compare the predictions of the deterministic approach with those of the two stochastic models, with respect both to sustained oscillations of the limit cycle type and to the influence of the proximity of a bifurcation point beyond which the system evolves to a stable steady state. The results indicate that robust circadian oscillations can occur even when the numbers of mRNA and nuclear protein involved in the oscillatory mechanism are reduced to a few tens or hundreds, respectively. The non-developed and developed versions of the stochastic model yield largely similar results and provide good agreement with the predictions of the deterministic model for circadian rhythms.

Key words: circadian rhythms, molecular noise, robustness, stochastic simulations

1. Introduction

To adapt to the natural periodicity of terrestrial environment characterized by the alternation of day and night, most living organisms, from cyanobacteria to mammals, have developed the capability of generating autonomously sustained oscillations with a period close to 24 h. These oscillations, known as circadian rhythms, are endogenous because they can occur in constant environmental conditions, e.g. constant darkness [1, 2]. During the last decade experimental advances have shed much light on the molecular mechanism of circadian rhythms [3]. Among the most prominent organisms that have been considered for such studies are the fly

Drosophila [4, 5] and the fungus *Neurospora* [3]. Molecular studies of circadian rhythms have since been extended to cyanobacteria, plants and mammals [6, 7]. The picture that emerges from these experiments is that in all cases investigated so far, the molecular mechanism of circadian oscillations relies on the negative autoregulation exerted by a protein on the expression of its gene [3–8].

A number of genes and their protein products involved in such a regulatory mechanism have been identified. Thus, in *Drosophila,* the proteins PER and TIM form a complex that indirectly represses the activation of the *per* and *tim* genes while in *Neurospora,* it is the FRQ protein that represses the expression of its gene *frq* [3–6]. The situation in mammals resembles that observed in *Drosophila,* but instead of TIM it is the CRY protein that forms a regulatory complex with a PER protein to inhibit the expression of the *per* genes [7]. Light can entrain circadian rhythms by inducing degradation of the TIM protein in *Drosophila,* and expression of the *frq* and *per* genes in *Neurospora* and mammals, respectively [3–7].

Based on these experimental observations a number of mathematical models for circadian rhythms have been proposed [9–15]. Such models generally take the form of a system of coupled ordinary differential equations. These deterministic models predict that in a certain range of parameter values the genetic regulatory network undergoes sustained oscillations of the limit cycle type corresponding to circadian rhythmic behavior, whereas outside this range the gene network operates in a stable steady state.

The number of molecules involved in the regulatory mechanism within the rhythm-producing cells is generally not known. The amount of interacting molecules taking part in circadian oscillations *in vivo* may well vary from a few thousands down to hundreds and even a few tens of protein or messenger RNA molecules. At such low concentrations it becomes necessary to resort to a stochastic approach. The purpose of this paper is to compare the predictions of deterministic and stochastic models for circadian oscillations.

We first consider in section 2 the deterministic version of a core model based on the negative regulation exerted by a protein on the expression of its gene. In section 3 we analyze two stochastic versions of this core molecular model for circadian rhythms. In the first version we introduce molecular noise without decomposing the deterministic mechanism into detailed reaction steps while in the second version we carry out such a detailed decomposition. The results of stochastic simulations performed by means of the Gillespie method [16, 17] are presented in section 4. We assess the robustness of circadian oscillations with respect to molecular noise and compare the predictions of the deterministic version of the model and of its two stochastic versions. We extend this comparison in section 5 by examining how the proximity from a bifurcation point influences the robustness of circadian oscillations with respect to molecular noise. Section 6 is devoted to a discussion of these results in regard to their significance both for cell physiology and for stochastic simulations.

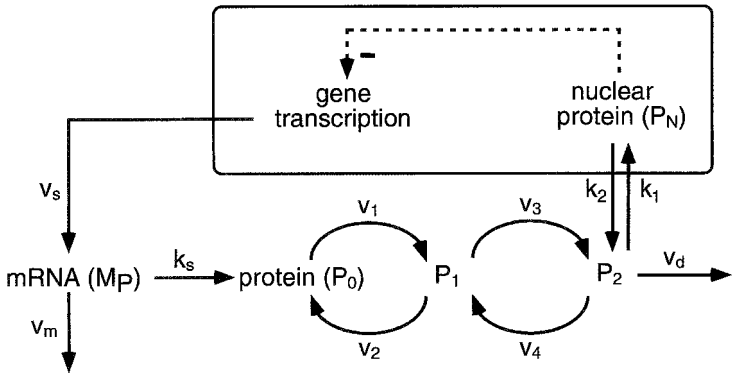

Figure 1. Core model for circadian rhythms. The model represents a prototype for the molecular mechanism of circadian oscillations based on negative autoregulation of gene expression. The model incorporates gene transcription, transport of mRNA (M_P) into the cytosol where it is translated into the protein (P_0) and degraded. The protein can be reversibly phosphorylated from the form P_0 into the forms P_1 and P_2, successively. The latter form is degraded or transported into the nucleus (P_N) where it exerts a negative feedback of cooperative nature on the expression of its gene. The model accounts for circadian oscillations of *per* mRNA and PER protein in *Drosophila*, and *frq* mRNA and FRQ protein in *Neurospora* [9, 10, 12]. Similar results are obtained for *Drosophila* in a more extended model incorporating the formation of a complex between the PER and TIM proteins [11–13]. The figure provides a scheme for the deterministic, 5-variable core model considered in section 2 for circadian oscillations, with indication of parameters characterizing the different steps [9, 10]: mRNA (M_P) is synthetized in the nucleus and transferred to the cytosol where it accumulates at a maximum rate v_s; there it is degraded by an enzyme of maximum rate v_m, and Michaelis constant K_m. The rate of synthesis of the protein P_0, proportional to M_P, is characterized by an apparent first-order rate constant k_s. Parameters v_i and K_i ($i = 1,\ldots,4$) denote the maximum rate and Michaelis constant of the kinase and phosphatase involved in the reversible phosphorylation of P_0 into P_1 and P_1 into P_2, respectively. The fully phosphorylated form P_2 is degraded by an enzyme of maximum rate v_d and Michaelis constant K_d, and transported into the nucleus at a rate characterized by the apparent first-order rate constant k_1. Transport of the nuclear form P_N into the cytosol is characterized by the apparent first-order rate constant k_2. The negative feedback exerted by P_N on gene transcription is described by an equation of the Hill type, in which n denotes the degree of cooperativity, and K_I the threshold constant for repression.

2. Deterministic Version of the Core Molecular Model for Circadian Oscillations

We consider a five-variable model previously proposed for circadian oscillations of the PER protein and *per* mRNA in *Drosophila* [9, 10], which also applies to oscillations of FRQ and *frq* mRNA in *Neurospora* [12]. The model, schematized in Figure 1, is based on the negative feedback exerted by a protein on the expression of its gene. The gene is first expressed in the nucleus and transcribed into messenger RNA (mRNA). The latter is transported into the cytosol where it is degraded and translated into the protein P_0. The protein (PER or FRQ) undergoes multiple phosphorylation, from P_0 into P_1 and from P_1 into P_2. These modifications, catalyzed

by a protein kinase, are reverted by a phosphatase. The fully phosphorylated form of the protein is marked up for degradation, and transported into the nucleus in a reversible manner. The nuclear form of the protein (P_N) represses the transcription of the gene.

In the model, the temporal variation of the concentrations of mRNA (M_P) and of the various forms of the regulatory protein, cytosolic (P_0, P_1, P_2) or nuclear (P_N), is governed by the following system of kinetic equations (see references 9 and 10 for further details):

$$\begin{aligned}
\frac{dM_P}{dt} &= v_s \frac{K_I^n}{K_I^n + P_N^n} - v_m \frac{M_P}{K_m + M_P} \\
\frac{dP_0}{dt} &= k_s M_P - v_1 \frac{P_0}{K_1 + P_0} + v_2 \frac{P_1}{K_2 + P_1} \\
\frac{dP_1}{dt} &= v_1 \frac{P_0}{K_1 + P_0} - v_2 \frac{P_1}{K_2 + P_1} - v_3 \frac{P_1}{K_3 + P_1} + v_4 \frac{P_2}{K_4 + P_2} \\
\frac{dP_2}{dt} &= v_3 \frac{P_1}{K_3 + P_1} - v_4 \frac{P_2}{K_4 + P_2} - v_d \frac{P_2}{K_d + P_2} - k_1 P_2 + k_2 P_N \\
\frac{dP_N}{dt} &= k_1 P_2 - k_2 P_N
\end{aligned} \tag{1}$$

The model accounts for the occurrence of sustained oscillations in continuous darkness. When taking into account the control of a parameter by light (e.g. the maximum protein degradation rate v_d in *Drosophila,* or the maximum rate of gene transcription v_s for *Neurospora*; see legend to Figure 1) the model also accounts for entrainment of circadian oscillations by light-dark cycles and for their phase-shifting by pulses of light. Similar results have been obtained in more detailed models incorporating additional clock gene products such as TIM and CLOCK [11–15].

The model of Figure 1 does not aim at representing the full, current view of the molecular mechanism of the circadian clock in *Drosophila, Neurospora* or mammals, which is known to involve a larger number of interacting proteins. Because the core model is simpler and contains a smaller number of variables, it is particularly well suited for stochastic simulations which, as will be shown below may require the decomposition of the deterministic mechanism into a large number of detailed reaction steps.

3. Two Stochastic Versions of the Core Molecular Model for Circadian Oscillations

To assess the effect of molecular noise we describe the reaction steps as stochastic birth and death processes [18]. Numerical simulations of the temporal evolution of

the genetic control system are performed by means of the Gillespie method [16, 17]. Besides other approaches [19–21], this method has been used to determine the dynamics of chemical [20, 21] biochemical [22] or genetic systems [23] in the presence of molecular noise. This method of the Monte-Carlo type associates a probability with each reaction step; at each time step the algorithm randomly determines the reaction that takes place according to its probability, as well as the time interval to the next reaction step. The numbers of molecules of the different reacting species as well as the probabilities are updated at each time step. In the approach proposed by Gillespie [16, 17] a parameter denoted Ω permits the modulation of the number of molecules present in the system. Using the Gillespie method we performed stochastic simulations of the core model described in section 2 by considering two versions of this model.

3.1. NON-DEVELOPED VERSION OF THE STOCHASTIC MODEL

The nonlinear terms appearing in the kinetic equations (1) do not correspond to single reaction steps. These terms rather represent compact kinetic expressions obtained after application of quasi-steady-state hypotheses on enzyme-substrate or gene-repressor complexes. The resulting expressions are of the Michaelis-Menten type for enzyme reaction rates or of the Hill type for cooperative binding of the repressor to the gene promoter. In the simplest stochastic version of the deterministic model of section 2, which we will refer to as the non-developed stochastic model, we attribute to each linear or nonlinear term of the kinetic equations a probability of occurrence of the corresponding reaction. These reactions and their associated probability are listed in Table I. Thus reaction 1 corresponds to the transcription of gene G into mRNA, M_P; the occurrence of this reaction with a probability w_1 results in increasing by one the number of molecules of M, without changing the number of gene molecules G which here remains equal to unity. Reaction 4 results in increasing by one the number of P_1 molecules and decreasing by one the number of molecules of P_0. The effect of the transitions brought about by the various reactions is listed in the last column in Table I.

In contrast to the treatment presented below in section 3.2, here we do not decompose the binding of the repressor P_N to the gene promoter into successive elementary steps, and rather retain the Hill function description for cooperative repression. A similar approach is taken for describing degradation of mRNA (reaction 2), translation of mRNA into protein (reaction 3), phosphorylation of P_0 into P_1 (reaction 4) and of P_1 into P_2 (reaction 6), as well as dephosphorylation of P_1 into P_0 (reaction 5) and of P_2 into P_1 (reaction 7), enzymatic degradation of P_2 (reaction 8), and reversible transport of P_2 into and out of the nucleus (reactions 9 and 10). Reactions 2 and 4–8 are of the Michaelian type, while reactions 3, 9 and 10 correspond to linear kinetics.

Table I. Non-detailed version of the stochastic model for circadian rhythms. The second column lists the sequence of reactions (see section 3.1). The probability of each reaction is given in the third column. The last column indicates the changes in the numbers of molecules taking part in the different reactions. The sequence of reactions corresponds to the mechanism underlying the deterministic core model governed by equations (1) and schematized in Figure 1.

Reaction number	Reaction	Probability of reaction	Transition
1	$G \longrightarrow M_P + G$	$w_1 = (v_s\Omega)\dfrac{(K_I\Omega)^n}{(K_I\Omega)^n + P_N^n}$	$M_P \longrightarrow M_P + 1$
2	$M_P \longrightarrow$	$w_3 = (v_m\Omega)\dfrac{M_P}{(K_m\Omega) + M_P}$	$M_P \longrightarrow M_P - 1$
3	$M_P \longrightarrow P_0 + M_P$	$w_2 = k_s M_P$	$P_0 \longrightarrow P_0 + 1$
4	$P_0 \longrightarrow P_1$	$w_4 = (v_1\Omega)\dfrac{P_0}{(K_1\Omega) + P_0}$	$P_0 \longrightarrow P_0 - 1$ $P_1 \longrightarrow P_1 + 1$
5	$P_1 \longrightarrow P_0$	$w_5 = (v_2\Omega)\dfrac{P_1}{(K_2\Omega) + P_1}$	$P_0 \longrightarrow P_0 + 1$ $P_1 \longrightarrow P_1 - 1$
6	$P_1 \longrightarrow P_2$	$w_6 = (v_3\Omega)\dfrac{P_1}{(K_3\Omega) + P_1}$	$P_1 \longrightarrow P_1 - 1$ $P_2 \longrightarrow P_2 + 1$
7	$P_2 \longrightarrow P_1$	$w_7 = (v_4\Omega)\dfrac{P_2}{(K_4\Omega) + P_2}$	$P_1 \longrightarrow P_1 + 1$ $P_2 \longrightarrow P_2 - 1$
8	$P_2 \longrightarrow$	$w_8 = (v_d\Omega)\dfrac{P_2}{(K_d\Omega) + P_2}$	$P_2 \longrightarrow P_2 - 1$
9	$P_2 \longrightarrow P_N$	$w_9 = k_1 P_2$	$P_2 \longrightarrow P_2 - 1$ $P_N \longrightarrow P_N + 1$
10	$P_N \longrightarrow P_2$	$w_{10} = k_2 P_N$	$P_2 \longrightarrow P_2 + 1$ $P_N \longrightarrow P_N - 1$

Table II. Detailed version of the stochastic model for circadian rhythms. The second column lists the sequence of reaction steps (see section 3.2). The probability of each reaction is given in the third column. The sequence of steps corresponds to the 10 reactions of the non-developed version of the model listed in Table I, and thus represents a detailed stochastic version of the core deterministic model governed by equations (1) and schematized in Figure 1. In the column listing the probability of occurrence of the detailed reaction steps, kinetic constants related to bimolecular reactions are scaled by Ω [16, 17]

Reaction number	Reaction step	Probability of reaction step
1a	$G + P_N \xrightarrow{a_1} GP_N$	$w_1 = a_1 \times G \times P_N/\Omega$
1b	$GP_N \xrightarrow{d_1} G + P_N$	$w_2 = d_1 \times GP_N$
1c	$GP_N + P_N \xrightarrow{a_2} GP_{N2}$	$w_3 = a_2 \times GP_N \times P_N/\Omega$
1d	$GP_{N2} \xrightarrow{d_2} GP_N + P_N$	$w_4 = d_2 \times GP_{N2}$
1e	$GP_{N2} + P_N \xrightarrow{a_3} GP_{N3}$	$w_5 = a_3 \times GP_{N2} \times P_N/\Omega$
1f	$GP_{N3} \xrightarrow{d_3} GP_{N2} + P_N$	$w_6 = d_3 \times GP_{N3}$
1g	$GP_{N3} + P_N \xrightarrow{a_4} GP_{N4}$	$w_7 = a_4 \times GP_{N3} \times P_N/\Omega$
1h	$GP_{N4} \xrightarrow{d_4} GP_{N3} + P_N$	$w_8 = d_4 \times GP_{N4}$
1i	$[G, GP_N, GP_{N2}, GP_{N3}] \xrightarrow{v_s} M_P$	$w_9 = v_s \times (G + GP_N + GP_{N2} + GP_{N3})$
2a	$M_P + E_m \xrightarrow{k_{m1}} C_m$	$w_{10} = k_{m1} \times M_P \times E_m/\Omega$
2b	$C_m \xrightarrow{k_{m2}} M_P + E_m$	$w_{11} = k_{m2} \times C_m$
2c	$C_m \xrightarrow{k_{m3}} E_m$	$w_{12} = k_{m3} \times C_m$
3	$M_P \xrightarrow{k_s} M_P + P_0$	$w_{13} = k_s \times M_P$
4a	$P_0 + E_1 \xrightarrow{k_{11}} C_1$	$w_{14} = k_{11} \times P_0 \times E_1/\Omega$
4b	$C_1 \xrightarrow{k_{12}} P_0 + E_1$	$w_{15} = k_{12} \times C_1$
4c	$C_1 \xrightarrow{k_{13}} P_1 + E_1$	$w_{16} = k_{13} \times C_1$
5a	$P_1 + E_2 \xrightarrow{k_{21}} C_2$	$w_{17} = k_{21} \times P_1 \times E_2/\Omega$
5b	$C_2 \xrightarrow{k_{22}} P_1 + E_2$	$w_{18} = k_{22} \times C_2$
5c	$C_2 \xrightarrow{k_{23}} P_0 + E_2$	$w_{19} = k_{23} \times C_2$
6a	$P_1 + E_3 \xrightarrow{k_{31}} C_3$	$w_{20} = k_{31} \times P_1 \times E_3/\Omega$

Table II. Continued

Reaction number	Reaction step	Probability of reaction step
6b	$C_3 \xrightarrow{k_{32}} P_1 + E_3$	$w_{21} = k_{32} \times C_3$
6c	$C_3 \xrightarrow{k_{33}} P_2 + E_3$	$w_{22} = k_{33} \times C_3$
7a	$P_2 + E_4 \xrightarrow{k_{41}} C_4$	$w_{23} = k_{41} \times P_2 \times E_4/\Omega$
7b	$C_4 \xrightarrow{k_{42}} P_2 + E_4$	$w_{24} = k_{42} \times C_4$
7c	$C_4 \xrightarrow{k_{43}} P_1 + E_4$	$w_{25} = k_{43} \times C_4$
8a	$P_2 + E_d \xrightarrow{k_{d1}} C_d$	$w_{26} = k_{d1} \times P_2 \times E_d/\Omega$
8b	$C_d \xrightarrow{k_{d2}} P_2 + E_d$	$w_{27} = k_{d2} \times C_d$
8c	$C_d \xrightarrow{k_{d3}} E_d$	$w_{28} = k_{d3} \times C_d$
9	$P_2 \xrightarrow{k_1} P_N$	$w_{29} = k_1 \times P_2$
10	$P_N \xrightarrow{k_2} P_2$	$w_{30} = k_2 \times P_N$

3.2. DEVELOPED VERSION OF THE STOCHASTIC MODEL

An alternative approach consists in developing explicitly the molecular regulatory mechanism schematized in Figure 1 into a sequence of detailed reaction steps. These steps are listed in Table II, together with their probability of occurrence denoted w_i (i = 1,... 30). The full sequence of steps listed in Table II will be referred to as the developed version of the stochastic model.

Reversible binding of the repressor to the gene promoter embedded into the transcription reaction 1 in the non-developed model (see Table I) is decomposed here into 8 steps (denoted 1a to 1h in Table II) in the case of cooperative binding of four molecules of P_N to the gene promoter G. Reaction 2 of Table I, which represents the enzymatic degradation of mRNA, is decomposed here into steps 2a–2c in Table II; these three steps represent, respectively, binding of M_P to enzyme E_m to form complex C_m, dissociation of C_m, and catalytic decomposition of C_m. Likewise, each of the other enzymatic processes, represented in Table I by a single, global reaction, is now represented by three steps, while the reactions characterized by linear kinetics remain represented by a single step.

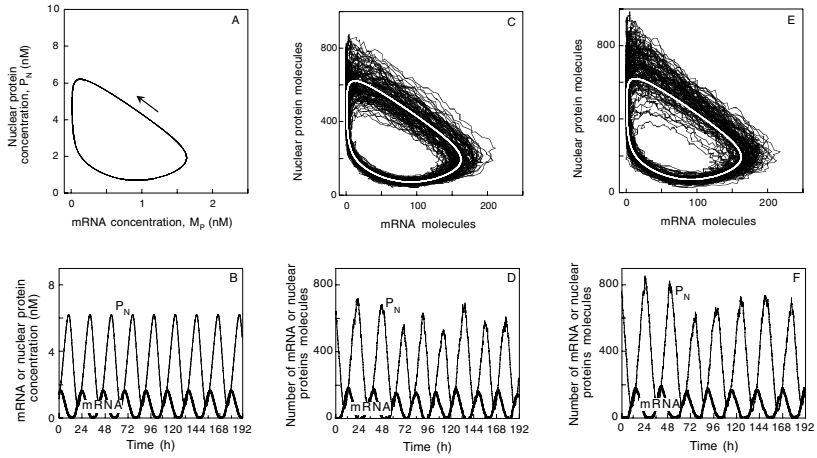

Figure 2. Sustained oscillations predicted by the deterministic and stochastic versions of the core model for circadian rhythms. (A) Limit cycle obtained in the 5-variable deterministic model governed by equations (1), shown as a projection onto the $P_N - M_P$ phase plane. (B) Sustained oscillations predicted by the deterministic model, corresponding to the limit cycle shown in panel A. (C) and (D) Limit cycle and sustained oscillations obtained for the non-developed version of the stochastic model (Table I). (E) and (F) Limit cycle and sustained oscillations obtained for the developed version of the stochastic model (Table II). The results in panels (C)-(F) are obtained numerically by means of the Gillespie method [16, 17]. As in the following figures stochastic simulations were performed for 2500 h, which corresponds to some 100 successive cycles. In (C) and (E) the deterministic limit cycle obtained in corresponding conditions (see panel A) is shown as a thick white curve; concentrations are transformed into numbers of molecules through multiplication by parameter Ω, which is equal to 100. Other parameter values are listed in Table III.

The effect of the transitions associated with each one of the detailed reaction steps (not shown in Table II) is similar to that listed in Table I: at each step, the number of molecules of species produced increases by one while the number of molecules consumed (or transported in the case of exchanges between the cytosol and the nucleus) decreases by one. In the case of transcription (step 1i) and translation (step 3), the number of gene and mRNA molecules, respectively, does not change in the course of the reaction.

4. Effect of Molecular Noise on Circadian Oscillations

Before dealing with the effect of molecular noise, we have to examine the predictions of the deterministic model governed by equations (1). Typical circadian oscillations predicted by this model are shown in Figure 2B. These oscillations correspond to the evolution toward a limit cycle (Figure 2A) shown here as a

Table III. Parameter values used for numerical simulations of the deterministic model and of its non-developed and developed stochastic versions in Figures 2–5. The reaction numbers refer to the corresponding lines in Tables I and II. In the last two columns, 'mol' means molecules. In the developed stochastic model, when varying Ω to modify the numbers of molecules involved in the circadian oscillatory mechanism, we wish to keep the number of gene promoter (G) equal to unity without altering the relative weights of the different probabilities w_i, so as to keep dynamic behavior consistent with that predicted by the corresponding deterministic model governed by equations (1). The numbers of enzyme molecules and the kinetic constants related to the steps involving G are therefore multiplied by Ω in the last column that lists the parameter values for the detailed model. In the same column, to allow for cooperativity of the repression process, the parameters a_j and d_j ($j = 1, \ldots, 4$) which appear in the detailed steps of reaction 1 (steps 1a–1h in Table II) are chosen so that the dissociation constant $K_j = d_j/a_j$ (with $K_I^4 = \Pi_{j=1}^4 K_j$) decreases as the number of molecules of P_N bound to the promoter increases

Reaction number	Deterministic model	Non-developed version of the stochastic model	Developed version of the stochastic model
1	$v_s = 0.5$ nMh^{-1} $K_I = 2$ nM $n = 4$	$v_s = 0.5$ mol h^{-1} $K_I = 2$ mol $n = 4$	$v_s = (0.5 \times \Omega)$ mol h^{-1}, $a_1 = \Omega$ mol^{-1} h^{-1}, $d_1 = (160 \times \Omega)$ h^{-1}, $a_2 = (10 \times \Omega)$ mol^{-1} h^{-1}, $d_2 = (100 \times \Omega)$ h^{-1}, $a_3 = (100 \times \Omega)$ mol^{-1} h^{-1}, $d_3 = (10 \times \Omega)$ h^{-1}, $a_4 = (100 \times \Omega)$ mol^{-1} h^{-1}, $d_4 = (10 \times \Omega)$ h^{-1}
2	$v_m = 0.3$ nMh^{-1} $K_m = 0.2$ nM	$v_m = 0.3$ mol h^{-1} $K_m = 0.2$ mol	$k_{m1} = 165$ mol^{-1} h^{-1}, $k_{m2} = 30$ h^{-1}, $k_{m3} = 3$ h^{-1}, $E_{mtot} = E_m + C_m = (0.1 \times \Omega)$ mol
3	$k_s = 2.0$ h^{-1}	$k_s = 2.0$ h^{-1}	$k_s = 2.0$ h^{-1}
4	$v_1 = 6.0$ nMh^{-1} $K_1 = 1.5$ nM	$v_1 = 6.0$ mol h^{-1} $K_1 = 1.5$ mol	$k_{11} = 146.6$ mol^{-1} h^{-1} $k_{12} = 200$ h^{-1}, $k_{13} = 20$ h^{-1} $E_{1tot} = E_1 + C_1 = (0.3 \times \Omega)$ mol
5	$v_2 = 3.0$ nMh^{-1} $K_2 = 2.0$ nM	$v_2 = 3.0$ mol h^{-1} $K_2 = 2.0$ mol	$k_{21} = 82.5$ mol^{-1} h^{-1}, $k_{22} = 150$ h^{-1}, $k_{23} = 15$ h^{-1}, $E_{2tot} = E_2 + C_2 = (0.2 \times \Omega)$ mol
6	$v_3 = 6.0$ nMh^{-1} $K_3 = 1.5$ nM	$v_3 = 6.0$ mol h^{-1} $K_3 = 1.5$ mol	$k_{31} = 146.6$ mol^{-1} h^{-1}, $k_{32} = 200$ h^{-1}, $k_{33} = 20$ h^{-1}, $E_{3tot} = E_3 + C_3 = (0.3 \times \Omega)$ mol
7	$v_4 = 3.0$ nMh^{-1} $K_4 = 2.0$ nM	$v_4 = 3.0$ mol h^{-1} $K_4 = 2.0$ mol	$k_{41} = 82.5$ mol^{-1} h^{-1}, $k_{42} = 150$ h^{-1}, $k_{43} = 15$ h^{-1}, $E_{4tot} = E_4 + C_4 = (0.2 \times \Omega)$ mol
8	$v_d = 1.5$ nMh^{-1} $K_d = 0.1$ nM	$v_d = 1.5$ mol h^{-1} $K_d = 0.1$ mol	$k_{d1} = 1650$ mol^{-1} h^{-1}, $k_{d2} = 150$ h^{-1}, $k_{d3} = 15$ h^{-1}, $E_{dtot} = E_d + C_d = (0.1 \times \Omega)$ mol
9	$k_1 = 2.0$ h^{-1}	$k_1 = 2.0$ h^{-1}	$k_1 = 2.0$ h^{-1}
10	$k_2 = 1.0$ h^{-1}	$k_2 = 1.0$ h^{-1}	$k_2 = 1.0$ h^{-1}

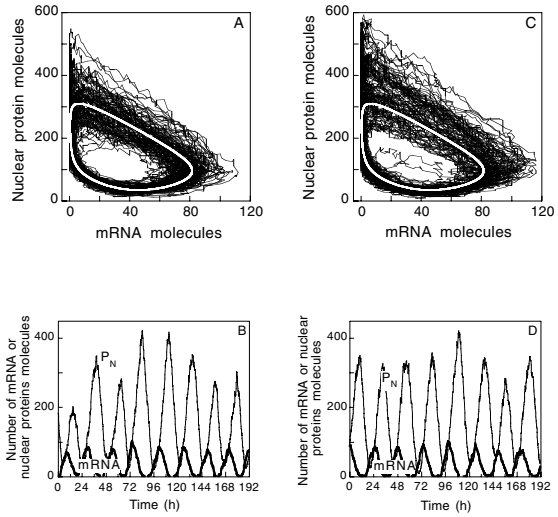

Figure 3. Robust circadian oscillations produced by the non-developed (B) and developed (D) versions of the stochastic model. The associated limit cycle trajectories are shown in (A) and (C), respectively, together with the deterministic limit cycle (thick white curve) obtained in corresponding conditions. Parameter values are as in Figure 2, except $\Omega = 50$.

projection onto the plane formed by the concentrations of mRNA (M_P) and nuclear protein (P_N).

Turning to the effect of noise, we now consider the dynamic behavior of the two stochastic versions of the core model for circadian rhythms. Shown in Figures 2C,D and 2E,F are the limit cycles and sustained oscillations of mRNA and nuclear regulatory protein obtained with the non-developed and developed versions of the stochastic model, respectively. For the sake of comparison, we have reproduced as a thick white trajectory in panels C and E of Figure 2 the limit cycle obtained in panel A for the deterministic model. The stochastic curves in Figure 2 have been obtained for $\Omega = 100$. For this value, the numbers of molecules of nuclear protein and mRNA vary in the range 50–800 and 0–200, respectively.

A first conclusion that can be drawn from the data presented in Figure 2 is that the circadian oscillatory behavior predicted by the deterministic model (panel B) is recovered when using either one of the two stochastic models for circadian rhythms (panels D and F). The mere effect of molecular noise is to increase the effective thickness of the limit cycle (panels C and E). A second conclusion is that both for the time series and for the limit cycle trajectory, the two stochastic versions of the model yield similar results. The same conclusions are drawn when considering stronger molecular noise at lower values of Ω, e.g. $\Omega = 50$ in Figure 3. There the numbers of molecules of nuclear protein and mRNA oscillate in the range 20–500 and 0–100, respectively. Robust circadian oscillations are still produced in both

versions of the stochastic model. The increased thickness of the limit cycle appears to be slightly greater in the case of the developed model (compare panels A and C in Figure 3).

5. Bifurcations and Molecular Noise

Much as in the case of the deterministic model, critical parameter values separate for the stochastic models regions in which the system undergoes sustained oscillations from regions where it evolves toward a stable steady state. Thus, for the deterministic model, sustained oscillations only occur in a domain bounded by two critical, bifurcation values of parameter v_d which measures the maximum rate of protein degradation. In the case of Figure 2A,B, sustained oscillations disappear below a value close to $v_d = 0.6$ nMh^{-1}. The stochastic simulations of both the non-developed (Figure 4) and developed (Figure 5) versions of the core model for circadian rhythms indicate that such bifurcation points also exist in the presence of molecular noise, even if the precise critical value of the control parameter may be difficult to localize because of the increased effect of noise near the bifurcation point (see panels C and E in Figures 4 and 5). Well below (Figures 4A,B and 5A,B) or above (Figures 4G,H and 5G,H) the bifurcation point, the genetic regulatory system evolves either to a stable steady state or to sustained oscillations of the limit cycle type, respectively. The behavior observed just above the bifurcation point (Figures 4E,F and 5E,F) is noisy but clearly differs from the low-amplitude fluctuations that occur around a stable steady state (Figures 4A,B and 5A,B).

Here again, for comparison, we have shown as a thick white line or point the attractor to which the deterministic model evolves in the phase plane. In Figures 4 and 5, this attractor is a stable steady state in (B) and (D), and a stable limit cycle in (F) and (H). Note that due to the proximity from the bifurcation point, the amplitude of the limit cycle is much reduced in (F), while damped oscillations (not shown) occur around the stable steady state in (D). This may explain why, in the presence of noise, dynamic behavior in (C) and (D) bears a strong resemblance to that observed in (E) and (F).

6. Discussion

The goal of this paper was to compare deterministic and stochastic models for circadian oscillations. In the presence of significant molecular noise, when the numbers of reacting molecules are small, stochastic simulations are needed. By means of such simulations we have shown that a core molecular mechanism for circadian rhythms based on negative autoregulation of gene expression can produce robust circadian oscillations, closely related to those obtained with the deterministic model, already when the maximum number of protein and mRNA molecules is in the hundreds or tens, respectively. The mean numbers of these molecules in the course of oscillations are smaller, because the levels of both protein and mRNA

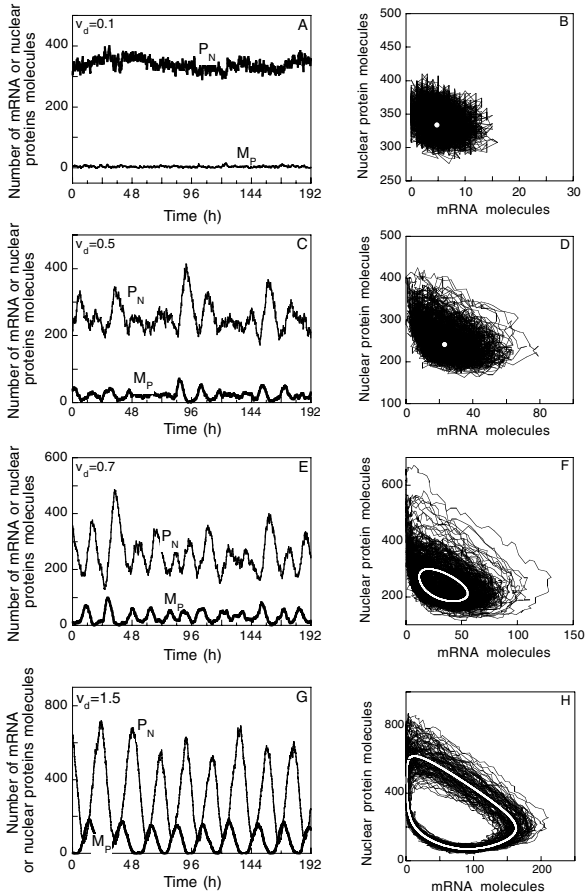

Figure 4. Effect of the proximity from a bifurcation point on the effect of molecular noise in the non-developed version of the stochastic model for circadian rhythms. The different panels are established for increasing values of parameter v_d (indicated in mol h^{-1}) that measures the maximum rate of protein degradation (see Figure 1 and Table I). The left panels represent the temporal evolution of the number of nuclear protein or mRNA molecules, while the right panels show the corresponding evolution in the phase plane. (A) and (B) Fluctuations around a stable steady state. (C) and (D) Fluctuations around a stable steady state for a value of v_d close to the bifurcation point which lies around 0.6 mol h^{-1}. Damped oscillations occur in these conditions when the system is displaced from the stable steady state. In (B) and (D) the white dot represents the stable steady state predicted by the deterministic version of the model in corresponding conditions. (E) and (F) Oscillations observed close to the bifurcation point. (G) and (H) Oscillations observed further from the bifurcation point, well into the domain of sustained oscillations. In (F) and (H) the thick white curve represents the limit cycle predicted by the deterministic version of the model governed by equations (1), in corresponding conditions, for the indicated values of v_d expressed in nMh^{-1}. The smaller amplitude of the limit cycle in (F) as compared to the limit cycle in (H) is associated with an increased influence of molecular noise (compare panels E and G). The curves are obtained by means of the Gillespie algorithm applied to the model of Table I. Parameter values are listed in Table III.

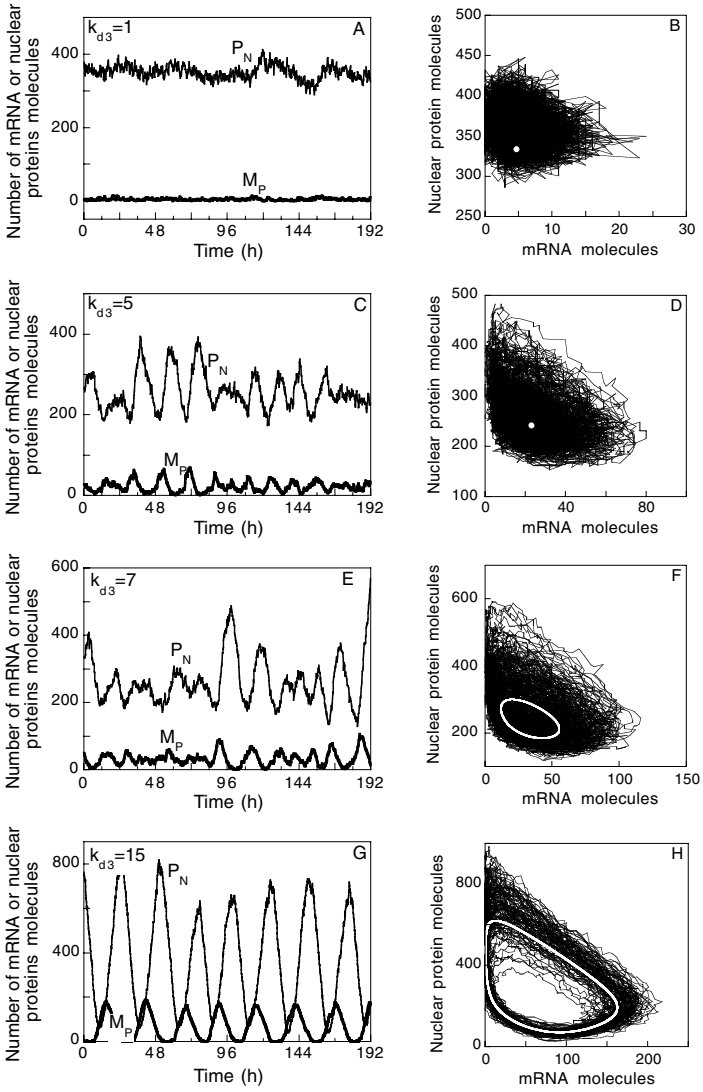

Figure 5. Effect of the proximity from a bifurcation point on the effect of molecular noise in the developed version of the stochastic model for circadian rhythms. The different panels are established for increasing values of parameter k_{d3} (indicated in h^{-1}) that measures the maximum rate of protein degradation (see step 8c in Table II). The significance of the curves is similar to that of the corresponding panels established in Figure 4 for the non-developed version of the stochastic model. The curves are obtained as in Figure 4 by means of the Gillespie algorithm applied to the model of Table II. Parameter values are listed in Table III.

can go down to very low values at the trough of the oscillations. Thus, in the cases considered in Figures 2F and 3D, the mean number of mRNA (nuclear protein) molecules is 67 (368) and 34 (194), respectively. It is only at very low numbers of molecules of protein and mRNA (reached, for example, for $\Omega = 10$) that noise begins to obliterate circadian rhythmicity [24].

The robustness of circadian oscillatory behavior in the presence of molecular noise has been quantified elsewhere by determining the half-time of the autocorrelation function and the standard deviation of the period of the oscillations [24]. Among the factors that appear to increase the robustness of circadian oscillations with respect to molecular noise are the cooperativity of repression [24], periodic forcing by light-dark cycles [24], and the formation of complexes between regulatory proteins (D. Forger and C. Peskin, personal communication).

A previous study of models based on negative autoregulation of gene expression reported a lack of robustness of circadian oscillations with respect to molecular noise [25]. The difference with respect to the results presented here and elsewhere [24] is likely due to the lower values considered for bimolecular rate constants characterizing the association of the repressor to the gene promoter. The authors of the contrasting report [25] used values bounded by the classical diffusion limit of 10^8 $M^{-1}s^{-1}$, while we chose larger values, in agreement with experimental observations that pertain to repressor binding to gene promoters [26]. However, we have obtained robust oscillations even at values of bimolecular rate constants lower than those considered in Figures 2 and 3.

We also compared the predictions of two stochastic versions of the core, 5-variable deterministic model for circadian oscillations. In the more compact version, we did not develop into elementary steps the enzymatic reactions described by Michaelis-Menten kinetics, nor the cooperative binding of the repressor to the gene promoter, described by a Hill function. The probability of occurrence of each of these reactions was taken as a product of a kinetic constant times the nonlinear function (see Table I), but the numbers of molecules in these expressions were allowed to vary in a stochastic manner. A similar approach has been followed in stochastic simulations of a model for intracellular Ca^{2+} oscillations [27]. In a second version, the reactions described by these nonlinear rate expressions were developed into a sequence of elementary steps. The non-developed version of the stochastic model thus contains 10 reaction steps (Table I), while the developed version contains 30 steps (Table II). Stochastic simulations of the two versions are in agreement both with respect to circadian oscillatory behavior (see Figures 2 and 3) and to the evolution toward a stable steady state when the value of the control parameter lies outside the critical range for sustained oscillatory behavior (Figures 4 and 5).

The results obtained here and in a previous study [24] with a core molecular model for circadian oscillations, as well as those obtained with a more extended model for circadian rhythms in *Drosophila* incorporating the formation of a complex between the PER and TIM proteins (D. Forger and C. Peskin, personal

communication, and Ref. 28, validate the predictions and the use of deterministic models for circadian rhythms. Moreover the present simulations indicate that when a stochastic approach is needed, the non-developed and developed stochastic versions of the deterministic model yield largely similar results.

Ackowledgements

This work was supported by grant n° 3.4607.99 from the *Fonds de la Recherche Scientifique Médicale* (F.R.S.M., Belgium). Support from the *Fondation D. & A. Van Buuren* to D. G. is also acknowledged. We wish to thank F. Baras, G. Dupont, D. Forger and P. Gaspard for fruitful discussions.

References

1. Moore-Ede, M.C., Sulzman, F.M. and Fuller, C.A.: *The Clocks that Time Us. Physiology of the Circadian Timing System,* Harvard Univ. Press, Cambridge, MA, 1982.
2. Edmunds, L.N. Jr.: *Cellular and Molecular Bases of Biological Clocks. Models and Mechanisms for Circadian Timekeeping,* Springer, New York, 1988.
3. Dunlap, J.C.: Molecular Bases for Circadian Clocks, *Cell* **96** (1999), 271–290.
4. Young, M.W.: Life's 24-hour Clock: Molecular Control of Circadian Rhythms in Animal Cells, *Trends Biochem. Sci.* **25** (2000), 601–606.
5. Williams, J.A. and Sehgal A.: Molecular Components of the Circadian System in *Drosophila, Annu. Rev. Physiol.* **63** (2001), 729–755.
6. Young, M.W. and Kay, S.A.: Time Zones: A Comparative Genetics of Circadian Clocks, *Nature Rev. Genetics* **2** (2001), 702–715.
7. Reppert, S.M. and Weaver D.R.: Molecular Analysis of Mammalian Circadian Rhythms, *Annu. Rev. Physiol.* **63** (2001), 647–676.
8. Hardin, P.E., Hall, J.C. and Rosbash, M.: Feedback of the *Drosophila* Period Gene Product on Circadian Cycling of its Messenger RNA Levels, *Nature* **343** (1990), 536–540.
9. Goldbeter, A.: A Model for Circadian Oscillations in the *Drosophila* Period Protein (PER), *Proc. R. Soc. Lond. B* **261** (1995), 319–324.
10. Goldbeter, A.: *Biochemical Oscillations and Cellular Rhythms. The Molecular Bases of Periodic and Chaotic Behaviour*, Cambridge Univ. Press, Cambridge, UK, 1996.
11. Leloup, J.-C. and Goldbeter, A.: A Model for Circadian Rhythms in *Drosophila* Incorporating the Formation of a Complex between the PER and TIM Proteins, *J. Biol. Rhythms* **13** (1998), 70–87.
12. Leloup, J.-C., Gonze, D. and Goldbeter, A.: Limit Cycle Models for Circadian Rhythms Based on Transcriptional Regulation in *Drosophila* and *Neurospora, J. Biol. Rhythms* **14** (1999), 433–448.
13. Leloup, J.-C. and Goldbeter, A.: Modeling the Molecular Regulatory Mechanism of Circadian Rhythms in *Drosophila, BioEssays* **22** (2000), 84–93.
14. Ueda, H.R., Hagiwara, M. and Kitano, H.: Robust Oscillations within the Interlocked Feedback Model of *Drosophila* Circadian Rhythm, *J. Theor. Biol.* **210** (2001), 401–406.
15. Smolen, P., Baxter, D.A. and Byrne, J.H.: Modeling Circadian Oscillations with Interlocking Positive and Negative Feedback Loops, *J. Neurosci.* **21** (2001), 6644–6656.
16. Gillespie, D.T.: A General Method for Numerically Simulating the Stochastic Time Evolution of Coupled Chemical Reactions, *J. Comput. Phys.* **22** (1976), 403–434.
17. Gillespie, D.T.: Exact Stochastic Simulation of Coupled Chemical Reactions, *J. Phys. Chem.* **81** (1977), 2340–2361.

18. Nicolis, G. and Prigogine, L: *Self-Organization in Nonequilibrium Systems*, Wiley, New York, 1977.
19. Morton-Firth, C.J. and Bray, D.: Predicting Temporal Fluctuations in an Intracellular Signalling Pathway, *J. Theor. Biol.* **192** (1998), 117–128.
20. Baras, F., Pearson, J.E. and Malek Mansour, M.: Microscopic Simulation of Chemical Oscillations in Homogeneous Systems, *J. Chem. Phys.* **93** (1990), 5747–5750.
21. Baras, F.: Stochastic Analysis of Limit Cycle Behaviour, In: L. Schimansky-Geier and T. Poeschel (eds.), *Stochastic Dynamics, Lecture Notes in Physics (LNP484)*, Springer-Verlag, Berlin, 1997, pp. 167–178.
22. McAdams, H.H. and Arkin, A.: Stochastic Mechanisms in Gene Expression, *Proc. Natl. Acad. Sci. USA* **94** (1997), 814–819.
23. Arkin, A., Ross, J. and McAdams, H.H.: Stochastic Kinetic Analysis of Developmental Pathway Bifurcation in Phage λ-Infected *Escherichia coli* Cells, *Genetics* **149** (1998), 1633–1648.
24. Gonze, D., Halloy, J. and Goldbeter, A.: Robustness of Circadian Rhythms with Respect to Molecular Noise, *Proc. Natl. Acad. Sci. USA* **99** (2002), 673–678.
25. Barkai, N. and Leibler, S.: Circadian Clocks Limited by Noise, *Nature* **403** (2000), 267–268.
26. von Hippel, P.H. and Berg, O.G.: Facilitated Target Location in Biological Systems, *J. Biol. Chem.* **264** (1989), 675–678.
27. Kraus, M., Lais, P. and Wolf, B.: Structured Biological Modelling: A Method for the Analysis and Simulation of Biological Systems Applied to Oscillatory Intracellular Calcium Waves, *BioSystems* **27** (1992), 145–169.
28. Gonze, D., Halloy, J., Leloup, J.C. and Goldbeter, A.: Stochastic models for circadian rhythms: effect of molecular noise on periodic and chaotic behavior. C.R. Biologies (2003), in press.